HHS Public Access

Author manuscript

J Immunol. Author manuscript; available in PMC 2022 June 01.

Published in final edited form as:

J Immunol. 2021 June 01; 206(11): 2521–2526. doi:10.4049/jimmunol.2100084.

Myosin 18A is a novel checkpoint regulator in B cell differentiation and antibody-mediated immunity

Michael B. Cheung[2], **Gospel Enyindah-Asonye**[2], **Ken Matsui**[2], **Ivan Kosik**[3], **Nina Dvorina**[2], **William M. Baldwin III**[2], **Jonathan W. Yewdell**[3], **Neetu Gupta**[2,*]

[2]Department of Inflammation and Immunity, Lerner Research Institute, Cleveland Clinic, Cleveland, Ohio, USA, [3]Laboratory of Viral Diseases, National Institute of Allergy and Infectious Diseases, National Institutes of Health, Bethesda, Maryland, USA

Abstract

We investigated the function of the newly discovered myosin family protein Myosin 18A (Myo18A) in antibody-mediated immunity by generating B cell-conditional Myo18A-deficient mice. Myo18A deficiency led to expansion of bone marrow progenitor B cells and mature B cells in secondary lymphoid organs. Myo18A-deficient mice displayed serum IgM hyperglobulinemia and increased splenic IgM secreting cells, with older mice switching to IgG1 hyperglobulinemia and autoantibody development. Immunization of Myo18A-deficient mice with inactivated influenza virus led to development of more potent neutralizing antibodies against the major antigen hemagglutinin, associated with persistent accumulation of antigen-specific germinal center B cells and more antigen-specific bone marrow plasma cells. *In vitro* stimulation with TLR7 and BCR ligands revealed a greater ability of Myo18A-deficient B cells to differentiate into antibody secreting cells, associated with higher AID and Blimp-1 expression. Overall, our study demonstrates that Myo18A is a novel negative regulator of B cell homeostasis, differentiation and humoral immunity.

INTRODUCTION

The B cell antibody response is tightly regulated to facilitate pathogen-specific immunity and prevent self-reactivity. Membrane and actin cytoskeleton dynamics play an important role in regulating B cell activation following crosslinking of the B cell receptor (BCR) by antigen (1–4). Ezrin, a membrane-cytoskeleton crosslinker, and Myosin 2A (Myo2A), the only conventional class II myosin expressed in lymphocytes, regulate BCR clustering (4), signal transduction (5–7), B cell antigen extraction, plasma cell differentiation, and humoral immune response (8–10).

The recently described class XVIII unconventional myosins are most closely related to Myo2A, and regulate important cellular processes in non-lymphoid cells (11–13). Myosin 18A (Myo18A) contains protein-protein interacting KE (Lysine-Glutamic acid) rich and

[*]**Correspondence to:** Neetu Gupta, Ph.D.; 9500 Euclid Avenue, NE40, Cleveland, OH 44195; guptan@ccf.org; Phone: (216) 444-7455; Fax: (216) 444-9329.

PDZ domains (domain contained within the proteins PSD95, Dlg1 and Zo-1), and an extended coiled-coil domain, the latter enabling homodimerization and interaction with Myo2A bipolar filaments (12, 14). We previously reported that Myo18A is expressed in both precursor and mature B cells, and interacts with ezrin, Myo2A and tyrosine phosphorylated proteins (15), suggesting that it may regulate physiological functions of B cells. Here, we show that Myo18A is a novel regulator that not only limits naïve B cell and immunoglobulin levels, but also restricts antigen-induced humoral immunity by restricting B cell differentiation into antibody secreting cells.

MATERIALS AND METHODS

Mice

Heterozygous Myo18A knockout first, conditional ready mice ($Myo18A^{FRT/+}$) were developed with KOMP (University of California, Davis) (MGI:4419827). Mice with floxed Myo18A alleles ($Myo18A^{FL/FL}$) were generated in house by crossing $Myo18A^{FRT/+}$ with ACTB:FLPe mice (Jackson labs) (16). B cell-specific conditional knockout mice (Myo18A BKO) were generated by crossing $Myo18A^{FL/FL}$ mice with $Mb1^{Cre/+}$ mice (17), and have the genotype $Myo18A^{FL/FL}$ $Mb1^{Cre/+}$. $Mb1^{Cre/+}$ mice, in which one Igα allele is replaced with the gene for Cre-recombinase, served as controls in all experiments. Experimental and control animals were not littermates or co-housed in the same cage. Male and female mice aged 2–3 months were used for flow cytometry and immunization experiments and 6–8-month-old mice for autoreactivity studies. All animal experiments were approved by the Cleveland Clinic Institutional Animal Care and Use Committee.

Virus, immunization and neutralization assay

Influenza A/Puerto Rico/8/1934 (PR8) (Mt. Sinai strain; H1N1) (18) was inactivated prior to immunization by exposure to UV. Mice were immunized i.p. with 2,500 hemagglutination activating units (HAUs) of UV-inactivated PR8 (UV-PR8) (18). Blood was collected from the tail vein prior to and weekly following immunization, and blood, spleen and bone marrow were collected for analysis. Virus neutralization assay was performed as described (19). The frequency of infected cells was normalized to a virus only control, and a non-linear regression curve was generated using the dose-response inhibition model to calculate the serum dilution factor leading to half maximal infection (50% neutralization dilution, ND_{50}), using Prism7 software (GraphPad).

Flow cytometry and western blotting

Purified B and T cells were isolated using MACS purification kits (Miltenyi Biotec) (Table S1). Western blotting for Myo18A was performed as previously described (15). B cell progenitors and subsets were identified from single cell suspensions of bone marrow, spleen and draining lymph nodes by staining with indicated antibodies and LIVE/DEAD stain (Table S1). Activation markers were analyzed on splenic $CD19^+$ B cells using specific antibodies (Table S1). Cells were acquired with a BD LSR Fortessa flow cytometer (BD Biosciences) and analyzed using FlowJo software (TreeStar) using established gating strategies (Fig. S1A–C). HA-specific B cells were identified using a PE-conjugated PR8 HA probe gifted by Dr. Troy Randall (University of Alabama, Birmingham) (20).

ELISA and ELISPOT

ELISA was performed to quantify total IgM, IgG, and IgG subclass (IgM, IgG, IgG1, IgG2b, IgG2c or IgG3) using indicated reagents (Table S1) as previously described (7). HA-specific IgM and IgG were measured using PR8 HA-coated ELISA plates (18). The area under the curve (AUC) was calculated for each serum sample using Prism 7 (GraphPad) software. IgM and IgG antibody secreting cells were quantified by ELISPOT as previously reported (7).

Autoantibody array

Serum samples from 6- to 8-month-old animals were analyzed at the University of Texas Southwestern Medical Center Microarray Core using autoantigen microarray panel 1, profiling 95 autoantigens and 8 internal controls. To quantify serum reactivity to autoantigens, the net fluorescent intensity (NFI) of each antigen was calculated by subtracting the local background and negative control. The signal-to-noise ratio (SNR) was calculated by subtracting the median background from the median foreground and dividing by the standard deviation of the background for each antigen. The autoantibody score (Ab-score), calculated as $\log_2((NFI*SNR) + 1)$, is depicted for both genotypes.

In vitro differentiation and qRT-PCR

Purified B cells were stimulated with 1 μg/ml Resiquimod (R848; InvivoGen) alone, or with 10 μg/ml goat anti-mouse IgM, μ chain specific $F(ab')_2$ (Jackson ImmunoResearch Laboratories) for 48 h, and IgM^+ ASCs quantified by ELISPOT assay. RNA was isolated from naïve and stimulated B cells, followed by cDNA synthesis, and qRT-PCR performed using the PowerUp SYBR Green Master Mix (Applied Biosystems) on a QuantStudio 5 Real-Time PCR system (Applied Biosystems). Gene expression was analyzed using forward and reverse primers (Table S1) for *Aicda* (AID), *Prdm1* (Blimp-1), and *Actb* (β-actin) (Integrated DNA Technologies). Expression was calculated by normalizing target gene expression to the housekeeping gene β-actin (ΔC_T), and calculating the relative fold induction of stimulated cells versus naïve B cells ($2^{-\Delta\Delta Ct}$).

Statistical analysis

Statistical significance was determined by calculating *P* values by two-sided unpaired *t* test unless otherwise stated. Significant differences between $Mb1^{Cre/+}$ and Myo18A BKO mice, with *P* values of less than 0.05, 0.01, 0.001 and 0.0001, are indicated as *, **, ***and ****, respectively. For all figures, mean ± SEM is shown and each symbol indicates an individual biological replicate. In Figure 4 statistically significant differences between mock, day 7, and day 28 UV-PR8 immunized mice are indicated with † for $Mb1^{Cre/+}$ mice and # for Myo18A BKO mice; where *P* values of less than 0.05, 0.01 and 0.001, are indicated as †/#, ††/## and †††/###, respectively. Data were plotted and analyzed using Prism 7 software (GraphPad).

RESULTS AND DISCUSSION

Myo18A regulates B cell development

To investigate the function of Myo18A in B cells we developed Myo18A$^{FRT/+}$ mice with one gene-trapped Myo18A allele (Fig. 1A). Breeding of heterozygous Myo18A$^{FRT/+}$ mice revealed a sub-Mendelian ratio of approximately $^{1}/_{3}^{rd}$ fully wild type and $^{2}/_{3}^{rd}$ heterozygotes (Table S2). Genotyping of embryos showed that systemic genetic deletion of Myo18A was embryonically lethal by day E9.5 (Table S2), consistent with reports in Drosophila (21, 22) and zebra fish (23, 24) where Myo18A is required to maintain myofiber integrity during development. Myo18A BKO mice were developed as described in Methods (Fig. 1A). B cell specificity of the Myo18A deletion was confirmed by immunoblotting of splenocytes, and purified B and T cells with an antibody specific to Myo18A (Fig. 1B). In humans, the 3' UTR of the *MYO18A* gene overlaps with the *TIAF1* gene (25). Although a homolog of *TIAF1* has not been annotated in the mouse genome, it is important to note that our knockout leaves the corresponding portion of the Myo18A gene intact. Therefore, the effects described here are because of Myo18A deletion alone. Nonetheless, there is a potential for differences between the regulation of and by Myo18A in mice and human B cells. As we have previously shown that B cell progenitors express Myo18A (15), we performed flow cytometry analysis of bone marrow cells from Mb1$^{Cre/+}$ and Myo18A BKO mice to investigate whether Myo18A deficiency affects B cell development. Myo18A BKO mice had increased bone marrow pro-pre-B cells, and immature B cells compared to Mb1$^{Cre/+}$ mice (Fig. 1C), whereas mature recirculating B cells were not altered (Fig. 1C). The expansion of B cell progenitors in the bone marrow suggests that Myo18A controls the earliest stages of B cell development in a B cell-intrinsic manner. Others have reported a link between increased Myo18A expression in bone marrow stromal cells and enhanced hematopoietic support (26). However, our data suggest a unique regulatory role for Myo18A in B cell progenitors that is distinct from the function attributed to it in bone marrow stromal cells. Cytokine signals from the microenvironment, such as IL-7 and thymic stromal lymphopoietin TLSP, and B cell intrinsic signals from the pre-BCR and BCR are all important in B cell development (27), and may be altered in Myo18A-deficient progenitors.

Myo18A regulates peripheral B cell homeostasis

We next evaluated the effect of Myo18A deletion on peripheral B cell and other immune cell populations. Myo18A BKO mice had a significant increase in the number of splenocytes compared to Mb1$^{Cre/+}$ controls (Fig. 1D) concomitant with elevated B cells and no change in T cell numbers (Fig. 1E, Fig. S1D). The follicular (Fo) B cell subset was significantly expanded in Myo18A BKO mice compared to Mb1$^{Cre/+}$ controls while marginal zone (MZ) B and total B1 B cells were not affected (Fig. 1F). Within the B1 B cell subset, however, the CD5^{+} B1a population was expanded in Myo18A BKO mice (Fig. 1G). Splenic B cells from Myo18A BKO mice had similar levels of surface immunoglobulins (Fig. S1E) and activation markers MHC-II, CD69, CD44, and CD80 (Fig. S1F). Myo18A BKO mice also had more cells in their lymph nodes (LNs) compared to Mb1$^{Cre/+}$ mice (Fig. 1H), and the number of both B and T cells was increased in LNs of Myo18A BKO mice (Fig. 1I). Elevated B cell numbers in both spleens and lymph nodes of Myo18A BKO mice suggests that Myo18A

expression in B cells regulates peripheral homeostasis, via higher bone marrow B cell output or increased B cell entry or retention in secondary lymphoid organs.

Hyperglobulinemia in Myo18A-deficient mice

To address if dysregulated numbers of peripheral B cells affect antibody production, we quantified serum immunoglobulins in $Mb1^{Cre/+}$ and Myo18A BKO mice. Serum IgM was significantly elevated in naïve 2- to 3-month-old Myo18A BKO mice compared to $Mb1^{Cre/+}$ (Fig. 2A) but IgG was not (Fig. 2B). To investigate if higher IgM was due to altered splenic antibody secretion capacity in Myo18A BKO mice we quantified antibody secreting plasma cells (PC) by flow cytometry and ELISPOT assay in naïve 2- to 3-month-old $Mb1^{Cre/+}$ and Myo18A BKO mice. Myo18A BKO mice had more PCs (Fig. 2C) and twice as many IgM secreting cells in their spleens compared to $Mb1^{Cre/+}$ mice (Fig. 2D). The number of IgG secreting ASCs also trended higher in Myo18A BKO mice compared to $Mb1^{Cre/+}$ mice (Fig. 2E). In contrast, bone marrow PCs (Fig. 2F), and IgM (Fig. 2G) and IgG (Fig. 2H) ASCs were similar in $Mb1^{Cre/+}$ and Myo18A BKO mice. These data demonstrate a higher overall antibody secretion capacity in Myo18A BKO mice, indicating that Myo18A regulates B cell differentiation into plasma cells in the spleens.

Myo18A-deficiency increases the generation of autoantibodies

We next examined if the hyperglobulinemia observed in 2–3-month-old mice persisted or worsened upon aging. Six-month-old Myo18A BKO mice did not show a difference in serum IgM concentrations (Fig. 3A) but had a significant increase in serum IgG compared to age-matched $Mb1^{Cre/+}$ mice (Fig. 3B). Quantification of IgG subclasses by ELISA showed higher IgG1 levels, with unaltered IgG2b, IgG2c, and IgG3 levels (Fig. 3C). Because naïve Myo18A BKO mice have elevated T cells in their lymph nodes, persistent B-T interactions may induce activation signals that lead to class switching. An accumulation of isotype switched B cells and IgG-secreting plasma cells may explain the elevation in IgG levels in 6-month-old Myo18A BKO mice. As elevated B cell numbers and serum IgG levels sometimes correlate with presence of autoreactive antibodies we employed an autoantigen array to quantify antibodies against 95 common self-antigens in the sera of 6-month-old $Mb1^{Cre/+}$ and Myo18A BKO mice. Overall, Myo18A BKO mice had significantly higher concentrations of autoreactive antibodies of both IgM (Fig. S2A) and IgG (Fig. S2B) isotype. IgM and IgG antibodies against a number of nuclear antigens including histone H2B, citrullinated histones, Smith antigen D2 (Sm D2), nucleolin, ribosomal phosphoprotein P1, and proliferating-cell nuclear antigen (PCNA) were increased in Myo18A BKO mice (Fig. 3D, E). Autoreactive antibodies against the extracellular matrix components fibrinogen S, citrullinated fibrinogen and aggrecan, were also significantly higher in Myo18A BKO mice (Fig. 3D, E). B1a B cells not only make much of the natural IgM (28), but also express autoreactive BCRs (29–31). Further, B1a B cells can switch from IgM to IgG expressing cells and differentiate into IgG-secreting cells (31, 32). Therefore, it is conceivable that expansion of $CD5^{+}$ B1a B cells in Myo18A BKO mice supports both, increase in serum IgM levels as well as IgM and IgG autoantibodies to self-antigens. While we did not observe higher autoantibodies to chromatin and dsDNA in Myo18A BKO mice, circulating antibodies to the lupus-associated Sm autoantigen were increased, (32, 33). Overt clinical signs of ongoing autoimmune or inflammatory disease, such as weight loss,

increased dermatitis, or swelling of joints and limbs, were not evident in the Myo18A BKO mice. Other pathological symptoms of autoimmunity, such as glomerular inflammation and deposition of IgG were also not observed in the Myo18A BKO mice. These data indicate that the deletion of Myo18A leads to increased expansion and differentiation of B1a B cells and increase in certain autoantibodies, but the progression to full blown autoimmune disease may require additional hits in the follicular B cell and T cell compartments.

Myo18A deficiency elicits a more robust antigen-specific B cell antibody response

Since the induction of antibody responses by follicular B cells are important for neutralization and clearance of viruses, we examined the effect of Myo18A deficiency on antigen-specific immunity by immunizing $Mb1^{Cre/+}$ and Myo18A BKO mice with UV-PR8. Compared to $Mb1^{Cre/+}$, Myo18A BKO mice developed higher serum anti-HA IgM (Fig. 4A), and anti-HA IgG (Fig. 4B). Day 28 sera from Myo18A BKO mice blocked *in vitro* infection of MDCK cells with live PR8 virus at higher serum dilutions than sera from $Mb1^{Cre/+}$, resulting in a significantly higher ND_{50} value (Fig. 4C). These data show that the deletion of Myo18A in B cells enables a stronger antigen-specific neutralizing antibody response to immunization. The greater neutralization capacity antiserum from immunized Myo18A BKO mice may result from a quantitative increase in HA-specific IgG, an increase in the affinity of such antibodies, and/or an increase in neutralizing antibodies against other flu antigens. We next examined the cellular basis for the stronger anti-HA antibody response in Myo18A BKO mice by performing flow cytometry analysis of spleen cells from mock immunized mice which received PBS, or mice immunized with UV-PR8 for 7 or 28 days. In all three groups, Myo18A BKO mice had more splenocytes than $Mb1^{Cre/+}$ mice (Fig. 4D). HA-specific B cells were elevated in UV-PR8 immunized Myo18A BKO mice relative to $Mb1^{Cre/+}$ mice on day 7, with further increase on day 28 (Fig. 4E). Greater expansion of HA-specific germinal center (GC) B cells was observed in Myo18A BKO mice after 7 days compared to $Mb1^{Cre/+}$ mice, and while $Mb1^{Cre/+}$ GC B cells contracted by 28 days, significantly higher numbers of HA^+ GC B cells persisted in Myo18A BKO spleens (Fig. 4F). Myo18A BKO mice had significantly more HA-specific IgG^+ ASCs in their bone marrow (Fig. 4G) than $Mb1^{Cre/+}$ mice, indicating an improved long-lived plasma cell response. Because naïve Myo18A-deficient B cells do not exhibit pre-existing activation prior to immunization (Fig. S1E, F), the increase in antigen-specific GC B cells suggests that either more B cells are activated post-immunization and entering the GC reaction, or there is greater expansion of B cells within the GC. Alternately, improved survival and persistence of B cells during GC selection may explain the observed increase in antigen-specific GC B cells I the later phase of the immune response.

Myo18A-deficient B cells exhibit greater differentiation

To determine the mechanism underlying enhanced humoral immunity observed in UV-PR8 immunized Myo18A BKO mice we modeled the response of splenic Myo18A-deficient B cells to R848, a TLR7/8 agonist and influenza virus ssRNA mimic, and anti-IgM, a surrogate for antigen *in vitro*. Increased IgM^+ ASCs were detected in B cells from Myo18A BKO mice compared with $Mb1^{Cre/+}$ upon stimulation for 48 h with R848 alone as well as with R848+anti-IgM (Fig. 4H). To delineate the molecular basis of increased differentiation, we analyzed the expression of key transcription factors AID and Blimp-1 in naïve and

R848+anti-IgM-stimulated B cells by qRT-PCR. Blimp-1 was induced upon stimulation of B cells of both genotypes by R848; however, Myo18A-deficient B cells displayed greater fold induction relative to naïve cells than did $Mb1^{Cre/+}$ B cells (Fig. 4I). Simultaneous TLR7 and BCR stimulation led to even greater expression of Blimp-1 but the expression was again significantly higher in Myo18A-deficient B cells (Fig. 4I). Similar results were obtained for the GC differentiation transcription factor AID (Fig. 4J). These data demonstrate that Myo18A restricts B cell differentiation to ASCs in a B cell-intrinsic manner, and that its deletion releases B cells from this inhibition.

Unconventional myosin family proteins have a vast array of functions in a variety of immune and non-immune cells (34). Here we report a novel role for the newest member of this family, Myo18A in B cell development, homeostasis, and antibody-mediated immunity. Conditional genetic deletion of Myo18A in B cells resulted in expansion of both developing and mature B cells, hyperglobulinemia, autoantibody development, persistent GC output and stronger neutralizing antibody response to influenza A virus. Taken together, our data demonstrate that Myo18A is a novel regulatory checkpoint protein whose absence leads to exaggerated B cell differentiation and antibody responses.

Supplementary Material

Refer to Web version on PubMed Central for supplementary material.

ACKNOWLEDGEMENTS

The authors acknowledge assistance from the University of Texas Southwestern Microarray Core facility.

This study was funded by an NIH grant (AI117350) to N.G.

Abbreviations used:

Myo18A BKO	Myosin 18A B cell conditional knockout
PR8	Influenza A/Puerto Rico/8/1934
UV-PR8	UV-inactivated PR8
ASC	antibody secreting cell

REFERENCES

1. Harwood NE, and Batista FD. 2010. Early events in B cell activation. Annu Rev Immunol 28: 185–210. [PubMed: 20192804]
2. Treanor B, Depoil D, Gonzalez-Granja A, Barral P, Weber M, Dushek O, Bruckbauer A, and Batista FD. 2010. The membrane skeleton controls diffusion dynamics and signaling through the B cell receptor. Immunity 32: 187–199. [PubMed: 20171124]
3. Tolar P 2017. Cytoskeletal control of B cell responses to antigens. Nat Rev Immunol 17: 621–634. [PubMed: 28690317]
4. Gupta N, Wollscheid B, Watts JD, Scheer B, Aebersold R, and DeFranco AL. 2006. Quantitative proteomic analysis of B cell lipid rafts reveals that ezrin regulates antigen receptor-mediated lipid raft dynamics. Nat Immunol 7: 625–633. [PubMed: 16648854]

5. Parameswaran N, Enyindah-Asonye G, Bagheri N, Shah NB, and Gupta N. 2013. Spatial coupling of JNK activation to the B cell antigen receptor by tyrosine-phosphorylated ezrin. J Immunol 190: 2017–2026. [PubMed: 23338238]

6. Treanor B, Depoil D, Bruckbauer A, and Batista FD. 2011. Dynamic cortical actin remodeling by ERM proteins controls BCR microcluster organization and integrity. J Exp Med 208: 1055–1068. [PubMed: 21482698]

7. Pore D, Parameswaran N, Matsui K, Stone MB, Saotome I, McClatchey AI, Veatch SL, and Gupta N. 2013. Ezrin tunes the magnitude of humoral immunity. J Immunol 191: 4048–4058. [PubMed: 24043890]

8. Vascotto F, Lankar D, Faure-Andre G, Vargas P, Diaz J, Le Roux D, Yuseff MI, Sibarita JB, Boes M, Raposo G, Mougneau E, Glaichenhaus N, Bonnerot C, Manoury B, and Lennon-Dumenil AM. 2007. The actin-based motor protein myosin II regulates MHC class II trafficking and BCR-driven antigen presentation. J Cell Biol 176: 1007–1019. [PubMed: 17389233]

9. Natkanski E, Lee WY, Mistry B, Casal A, Molloy JE, and Tolar P. 2013. B cells use mechanical energy to discriminate antigen affinities. Science 340: 1587–1590. [PubMed: 23686338]

10. Hoogeboom R, Natkanski EM, Nowosad CR, Malinova D, Menon RP, Casal A, and Tolar P. 2018. Myosin IIa Promotes Antibody Responses by Regulating B Cell Activation, Acquisition of Antigen, and Proliferation. Cell Rep 23: 2342–2353. [PubMed: 29791846]

11. Berg JS, Powell BC, and Cheney RE. 2001. A millennial myosin census. Mol Biol Cell 12: 780–794. [PubMed: 11294886]

12. Furusawa T, Ikawa S, Yanai N, and Obinata M. 2000. Isolation of a novel PDZ-containing myosin from hematopoietic supportive bone marrow stromal cell lines. Biochem Biophys Res Commun 270: 67–75. [PubMed: 10733906]

13. Mori K, Furusawa T, Okubo T, Inoue T, Ikawa S, Yanai N, Mori KJ, and Obinata M. 2003. Genome structure and differential expression of two isoforms of a novel PDZ-containing myosin (MysPDZ) (Myo18A). J Biochem 133: 405–413. [PubMed: 12761286]

14. Billington N, Beach JR, Heissler SM, Remmert K, Guzik-Lendrum S, Nagy A, Takagi Y, Shao L, Li D, Yang Y, Zhang Y, Barzik M, Betzig E, Hammer JA 3rd, and Sellers JR. 2015. Myosin 18A coassembles with nonmuscle myosin 2 to form mixed bipolar filaments. Curr Biol 25: 942–948. [PubMed: 25754640]

15. Matsui K, Parameswaran N, Bagheri N, Willard B, and Gupta N. 2011. Proteomics analysis of the ezrin interactome in B cells reveals a novel association with Myo18aα. J. Proteome Res 10: 3983–3992. [PubMed: 21751808]

16. Rodriguez CI, Buchholz F, Galloway J, Sequerra R, Kasper J, Ayala R, Stewart AF, and Dymecki SM. 2000. High-efficiency deleter mice show that FLPe is an alternative to Cre-loxP. Nat Genet 25: 139–140. [PubMed: 10835623]

17. Hobeika E, Thiemann S, Storch B, Jumaa H, Nielsen PJ, Pelanda R, and Reth M. 2006. Testing gene function early in the B cell lineage in mb1-cre mice. Proc Natl Acad Sci U S A 103: 13789–13794. [PubMed: 16940357]

18. Angeletti D, Gibbs JS, Angel M, Kosik I, Hickman HD, Frank GM, Das SR, Wheatley AK, Prabhakaran M, Leggat DJ, McDermott AB, and Yewdell JW. 2017. Defining B cell immunodominance to viruses. Nat. Immunol 18: 456–463. [PubMed: 28192417]

19. Kosik I, Angeletti D, Gibbs JS, Angel M, Takeda K, Kosikova M, Nair V, Hickman HD, Xie H, Brooke CB, and Yewdell JW. 2019. Neuraminidase inhibition contributes to influenza A virus neutralization by anti-hemagglutinin stem antibodies. J Exp Med 216: 304–316. [PubMed: 30683737]

20. Allie SR, Bradley JE, Mudunuru U, Schultz MD, Graf BA, Lund FE, and Randall TD. 2019. The establishment of resident memory B cells in the lung requires local antigen encounter. Nat Immunol 20: 97–108. [PubMed: 30510223]

21. Ivanov AI, Rovescalli AC, Pozzi P, Yoo S, Mozer B, Li HP, Yu SH, Higashida H, Guo V, Spencer M, and Nirenberg M. 2004. Genes required for Drosophila nervous system development identified by RNA interference. Proc Natl Acad Sci U S A 101: 16216–16221. [PubMed: 15534205]

22. Bonn BR, Rudolf A, Hornbruch-Freitag C, Daum G, Kuckwa J, Kastl L, Buttgereit D, and Renkawitz-Pohl R. 2013. Myosin heavy chain-like localizes at cell contact sites during Drosophila

myoblast fusion and interacts in vitro with Rolling pebbles 7. Exp Cell Res 319: 402–416. [PubMed: 23246571]

23. Cao J, Li S, Shao M, Cheng X, Xu Z, and Shi D. 2014. The PDZ-containing unconventional myosin XVIIIA regulates embryonic muscle integrity in zebrafish. J Genet Genomics 41: 417–428. [PubMed: 25160974]
24. Cao JM, Cheng XN, Li SQ, Heller S, Xu ZG, and Shi DL. 2016. Identification of novel MYO18A interaction partners required for myoblast adhesion and muscle integrity. Sci Rep 6: 36768. [PubMed: 27824130]
25. Chang NS, Mattison J, Cao H, Pratt N, Zhao Y, and Lee C. 1998. Cloning and characterization of a novel transforming growth factor-beta1-induced TIAF1 protein that inhibits tumor necrosis factor cytotoxicity. Biochem. Biophys. Res. Commun 253: 743–749. [PubMed: 9918798]
26. Furusawa T, Ikawa S, Yanai N, and Obinata M. 2000. Isolation of a Novel PDZ-Containing Myosin from Hematopoietic Supportive Bone Marrow Stromal Cell Lines. Biochem. Biophys. Res. Commun 270: 67–75. [PubMed: 10733906]
27. Carsetti R 2000. The development of B cells in the bone marrow is controlled by the balance between cell-autonomous mechanisms and signals from the microenvironment. J Exp Med 191: 5–8. [PubMed: 10620600]
28. Lalor PA 1991. An Evolutionarily-Conserved Role for Murine Ly-1 B Cells in Protection Against Bacterial Infections. Autoimmunity 10: 71–76. [PubMed: 1742426]
29. Deng J, Wang X, Chen Q, Sun X, Xiao F, Ko K-H, Zhang M, and Lu L. 2016. B1a cells play a pathogenic role in the development of autoimmune arthritis. Oncotarget; *Vol* 7, *No* 15.
30. Hoffmann A, Kerr S, Jellusova J, Zhang J, Weisel F, Wellmann U, Winkler TH, Kneitz B, Crocker PR, and Nitschke L. 2007. Siglec-G is a B1 cell–inhibitory receptor that controls expansion and calcium signaling of the B1 cell population. Nat. Immunol 8: 695–704. [PubMed: 17572677]
31. Diana J, Simoni Y, Furio L, Beaudoin L, Agerberth B, Barrat F, and Lehuen A. 2013. Crosstalk between neutrophils, B-1a cells and plasmacytoid dendritic cells initiates autoimmune diabetes. Nat. Med 19: 65–73. [PubMed: 23242473]
32. Enghard P, Humrich JY, Chu VT, Grussie E, Hiepe F, Burmester G-R, Radbruch A, Berek C, and Riemekasten G. 2010. Class switching and consecutive loss of dsDNA-reactive B1a B cells from the peritoneal cavity during murine lupus development. Eur. J. Immunol 40: 1809–1818. [PubMed: 20333624]
33. McClain MT, Ramsland PA, Kaufman KM, and James JA. 2002. Anti-Sm Autoantibodies in Systemic Lupus Target Highly Basic Surface Structures of Complexed Spliceosomal Autoantigens. J Immunol 168: 2054. [PubMed: 11823543]
34. Maravillas-Montero JL, and Santos-Argumedo L. 2012. The myosin family: unconventional roles of actin-dependent molecular motors in immune cells. J Leukoc Biol 91: 35–46. [PubMed: 21965174]

KEY POINTS

1. Myo18A maintains the number of progenitor and mature B cells
2. Myo18A restricts B cell differentiation into antibody secreting cells
3. Myo18A regulates autoreactive and antigen-specific B cell antibody responses

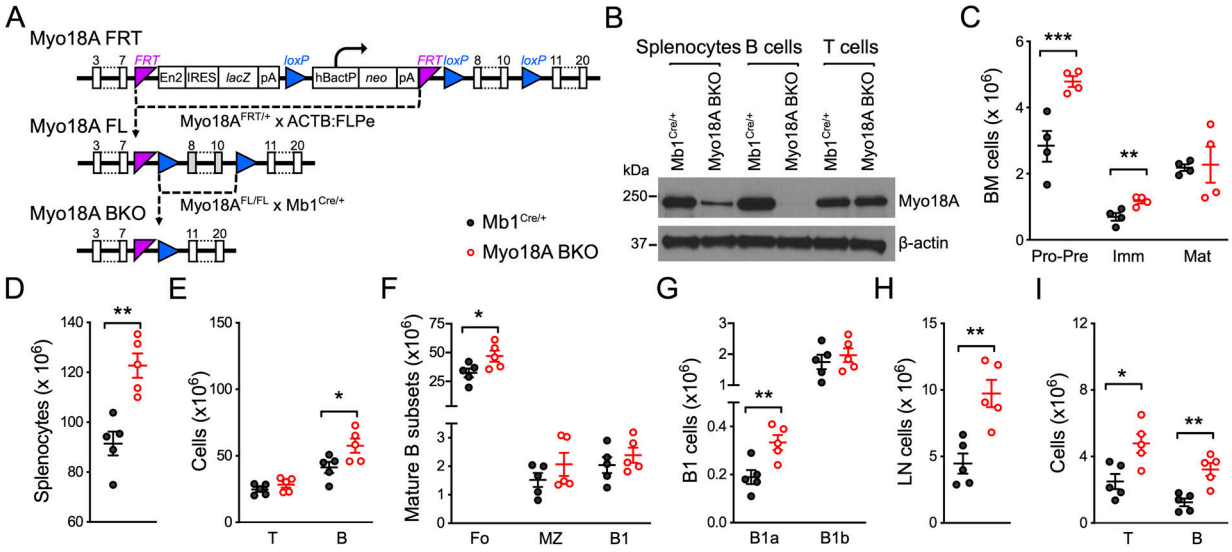

Figure 1. B cell-specific deletion of Myo18A leads to expansion of bone marrow B cell progenitors and peripheral B cell subsets.

(A) Strategy for development of B cell-specific Myo18A conditional knockout (Myo18A BKO). **(B)** Lysates from $Mb1^{Cre/+}$ and Myo18A BKO splenocytes, B cells, and T cells probed for Myo18A and β-actin. **(C)** Bone marrow progenitor (Pro-Pre, $B220^{lo}IgM^{-}$), immature (Imm, $B220^{lo}IgM^{+}$) and recirculating mature (Mat, $B220^{hi}IgM^{+}$) B cell populations in 2- to 3-month-old $Mb1^{Cre/+}$ and Myo18A BKO mice. **(D-G)** Number of splenocytes (D), $CD19^{+}$ B cells and $CD3^{+}$ T cells (E), splenic follicular (Fo: $CD19^{+}CD93^{-}CD23^{+}CD21^{int}$), marginal zone (MZ: $CD19^{+}CD93^{-}CD23^{-}CD21^{hi}$) and B1 B cells ($CD19^{+}$ $CD93^{-}CD23^{-}CD21^{-}$) (F), and $CD5^{+}$ B1a and $CD5^{-}$ B1b cells (G) in naïve 2- to 3-month old $Mb1^{Cre/+}$ and Myo18A BKO mice. **(H-I)** Number of lymph node (LN) cells (H), and B and T cells (I). n = 4 per genotype for C, and 5 per genotype for D-I. Representative data from 2–4 experiments.

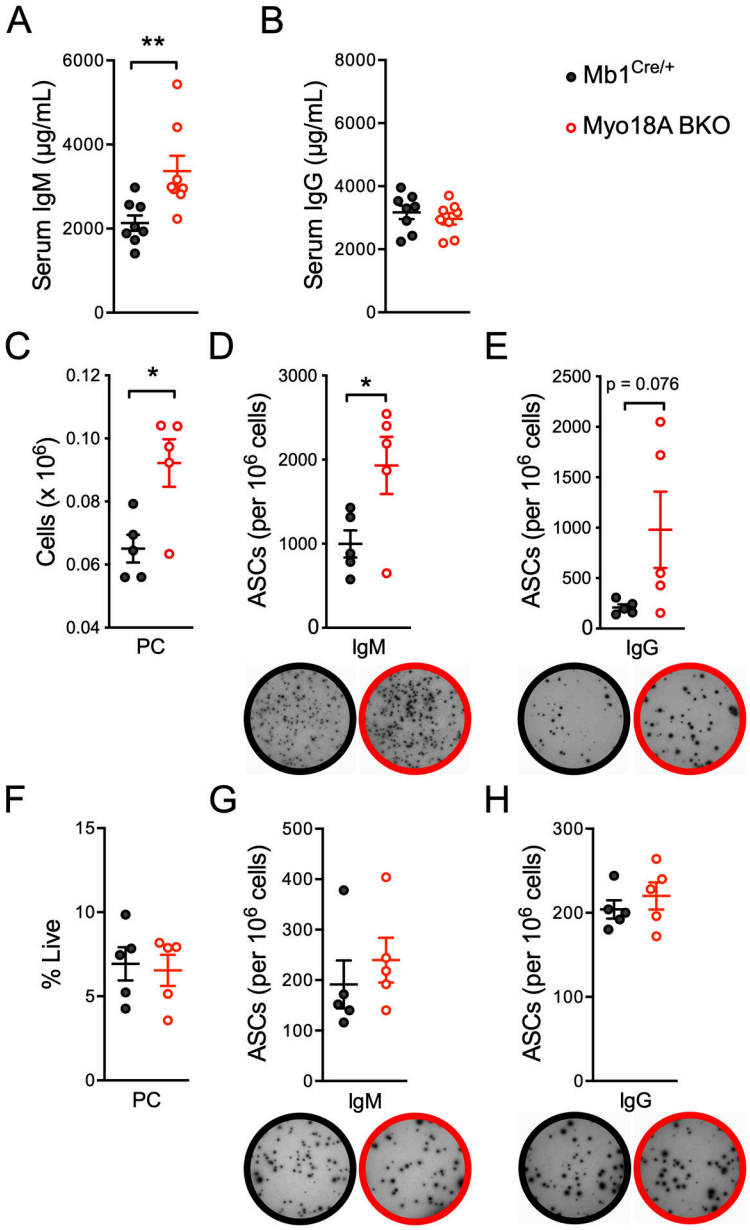

Figure 2. Deletion of Myo18A results in hyperglobulinemia.

(A-B) Serum concentration of total IgM (A) and IgG (B) in naïve 2- to 3-month old $Mb1^{Cre/+}$ and Myo18A BKO mice. **(C)** Number of $CD19^{-}B220^{lo}CD138^{+}$ splenic plasma cells (PC). **(D-E)** ELISPOT assay for IgM^{+} (D) and IgG^{+} (E) antibody secreting cells (ASCs) quantified as ASCs per million splenocytes. **(F)** Number of $CD19^{-}B220^{lo}CD138^{+}$ bone marrow plasma cells (PC). **(G-H)** ELISPOT assay for IgM^{+} (G) and IgG^{+} (H) antibody secreting cells (ASCs) quantified as ASCs per million bone marrow cells. n=8 per genotype for A-B, and 5 per genotype for C-H. Representative data from 2–5 experiments.

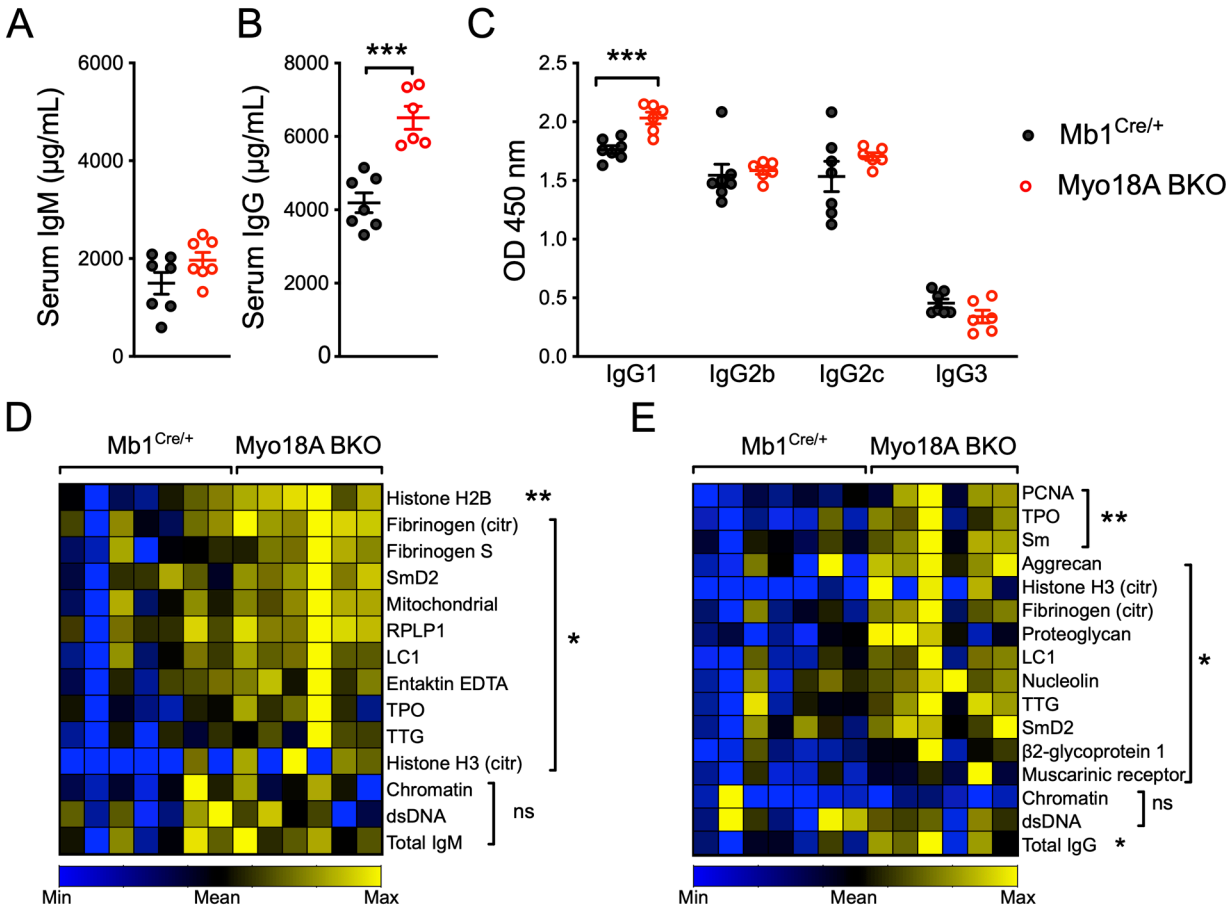

Figure 3. Myo18A-deficiency leads to development of self-reactive antibodies.

(A-C) Serum concentration of IgM (A), IgG (B), and IgG subclasses IgG1, IgG2b, IgG2c, and IgG3 (C) in 6- to 8-month old $Mb1^{Cre/+}$ and Myo18A BKO mice. **(D-E)** Heatmaps of normalized Ab-score data for IgM- (D) and IgG-reactive (E) autoantigens in $Mb1^{Cre/+}$ and Myo18A BKO mice. n = 6–7 mice per genotype. Representative data from 3 experiments.

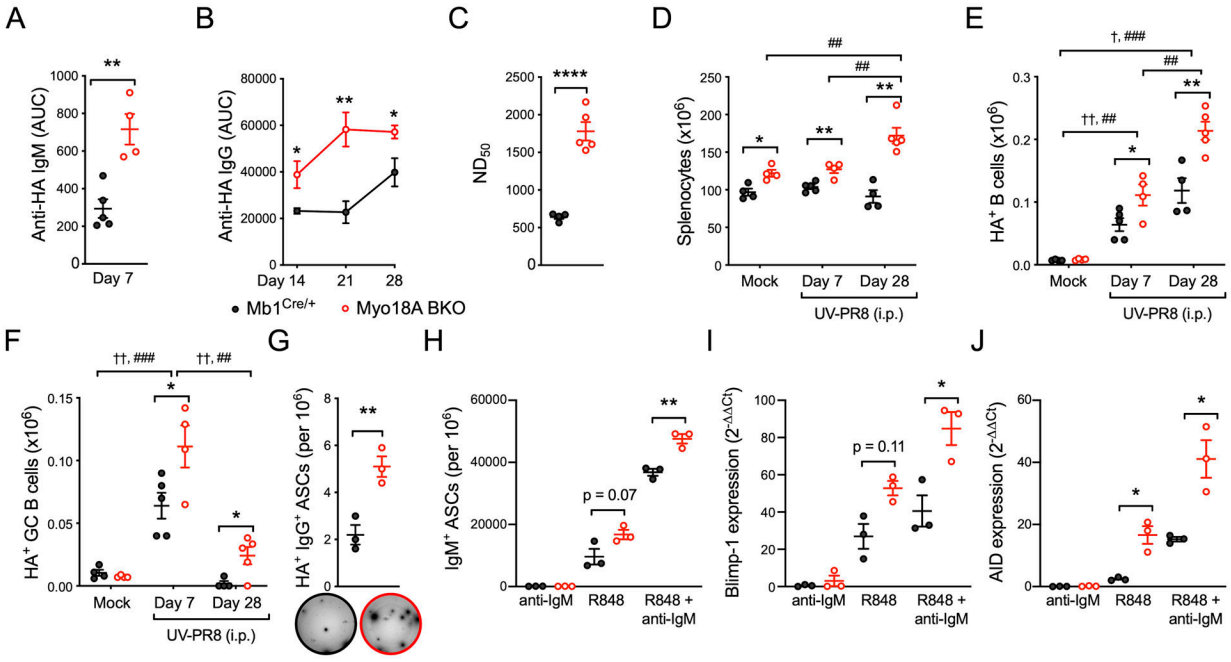

Figure 4. Deletion of Myo18A promotes more robust flu virus-specific cellular and antibody response by enhancing B cell differentiation.

Serum anti-PR8 HA IgM **(A)** and IgG **(B)** in immunized $Mb1^{Cre/+}$ and Myo18A BKO in quantified as area under the curve (AUC). **(C)** Neutralization capacity of day 28 serum expressed as 50% neutralization dilution (ND_{50}). **(D-G)** Number of splenocytes (D) HA^+CD19^+ B cells (E), $HA^+CD19^+GL7^+CD95^+$ GC B cells (F), and HA^+IgG^+ ASCs (G) in $Mb1^{Cre/+}$ and Myo18A BKO mice immunized with UV-inactivated PR8. **(H-J)** Differentiation of B cells *in vitro* assessed by ELISPOT for IgM^+ ASCs (H), and Blimp-1 (I) and AID (J) gene expression, in 48 h cultures of R848 and anti-IgM-stimulated B cells from $Mb1^{Cre/+}$ and Myo18A BKO mice. n = 4–5 per genotype for A-F, and 3 for G-J. Representative data from 1–3 experiments.